

Computational band-structure engineering of III–V semiconductor alloys

Clint B. Geller

Bettis Atomic Power Laboratory, West Mifflin, Pennsylvania 15122

Walter Wolf

Materials Design, Oceanside, California 92057 and Le Mans, France

Silvia Picozzi and Alessandra Continenza

Istituto Nazionale di Fisica della Materia (INFN), Dipartimento di Fisica, Università degli Studi di L'Aquila, Coppito, Italy

Ryoji Asahi,^{a)} Wolfgang Mannstadt, and Arthur J. Freeman

Department of Physics and Astronomy and Materials Research Center, Northwestern University, Evanston, Illinois 60201

Erich Wimmer^{b)}

Materials Design and Institut Supérieur des Matériaux du Mans (ISMANS), Le Mans, France

(Received 20 November 2000; accepted for publication 11 May 2001)

Accurate band structures of binary semiconductors AB (A=Al, Ga, In and B=P, As, Sb) and selected ternary III–V semiconductors were calculated using an all-electron screened exchange approach within the full potential linearized augmented plane-wave method. Fundamental band gaps and Γ – L and Γ – X separations in higher-lying conduction bands are predicted with an accuracy of a few tenths of 1 eV. Screened exchange also performs better than the local density approximation for calculating conduction-band effective masses. Highly n -doped InPAs materials with compositions near InP_{0.2}As_{0.8} offer lower effective masses, greater optical band-gap shifts, and potentially higher electron mobility than n -doped InGaAs materials with comparable band gaps.
© 2001 American Institute of Physics. [DOI: 10.1063/1.1383282]

Using concepts such as screened exchange (sX),^{1–3} efficient and accurate first-principles band-gap calculations recently have become possible for a wide range of semiconductors. However, it is not clear how well the sX approach predicts higher-lying conduction bands, which are important, for example, in the prediction of optical properties. In addition, ternary and quaternary semiconductor alloy systems including In_{1–x}Ga_xAs, InP_yAs_{1–y}, and In_{1–x}Ga_xAs_{1–y}Sb_y are employed in thermophotovoltaic (TPV) devices both as active layers and/or spectral control filter materials.^{4,5} An accurate knowledge of conduction-band topology enables the identification of alloy compositions where maximum carrier mobility and lifetime are likely to be found for specific band-gap and lattice parameter ranges. Major influences on carrier effective mass, mobility, and lifetime are the positions and shape of the conduction band (CB) secondary minima most often found at the point $L(111)$ in the Brillouin zone. The effect of CB side valleys is also illustrated by the Gunn effect,^{6,7} and by recent experiments on nonequilibrium phonon dynamics in InP and InAs.⁸

A further consideration is that the active layers of photovoltaic devices and diodes may be heavily doped. Since dispersion near the CB minimum is extreme in many III–V compounds [InAs has an electron effective mass ratio of 0.023 (Ref. 9)], the carrier effective masses of heavily n -doped III–V materials tend to depend strongly on carrier concentration. Thus, the collective behavior of the free carriers can be influenced by the curvature of the conduction

band at points far from Γ . The presence of a low-lying conduction-band side valley at L or at X can significantly alter the conduction-band dispersion around the central minimum, affecting carrier effective masses, optical band gaps (i.e., Moss–Burstein shifts), and plasma frequencies, among other properties. It is then clear that a detailed, quantitative understanding of conduction-band dispersion in semiconductors can aid the design of optoelectronic materials.

In the current study, energy-band structures and excitation energies were calculated within the screened exchange method^{1,2} as implemented recently^{10,11} in the full-potential linearized augmented plane-wave (FLAPW) method.^{12,13} The resulting sX-FLAPW method is a significant extension of the standard density functional formalism based on the local density approximation (LDA) whose utility was restricted chiefly to ground-state properties. The sX-FLAPW approach allows one to predict quasiparticle energies (band structures) that can be interpreted as excitation energies.

Concerning the fundamental band gap, typical deviations between experimental values and sX-FLAPW predictions¹⁰ are a few tenths of 1 eV, as shown in Fig. 1. Critically for applications such as TPV, the relative error of the method is the same for wide and narrow band gaps.

The applicability of the sX approach to higher-lying states had not been well established and is demonstrated here by investigating (i) Γ – L and Γ – X separations (i.e., the energy difference between the CB minima at Γ , L , and X , respectively) and (ii) effective masses for III–V semiconductors of type AB (A=Al, Ga, In and B=P, As, Sb). The sX-FLAPW results are compared to LDA values and experimental data summarized in Tables I (Refs. 14–17) and II (Ref. 18).

^{a)}Present address: Toyota Central R&D Labs., Inc., Nagakute Aichi 480-1192, Japan.

^{b)}Electronic mail: ewimmer@materialsdesign.com

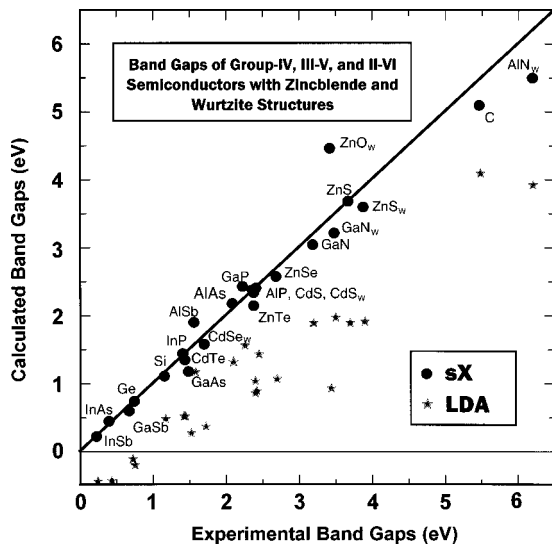


FIG. 1. Calculated vs experimental energy-band gaps for 24 elemental and binary semiconductors. Results from sX-FLAPW calculations are shown as solid circles. Values obtained with the conventional local density approximation (LDA) are represented as stars. Note the larger scatter of the LDA results and the qualitative failure of LDA for narrow-band-gap materials.

The $\Gamma-L$ and $\Gamma-X$ separations (cf. Table I) show an overall better performance of sX compared with LDA. A remarkable case is the $\Gamma-L$ separation in InAs. The most often reported experimental value is 0.74 eV,¹⁵ whereas sX gives 1.21 eV. Recent measurements, by using improved techniques, resulted in a revised value of 1.10 ± 0.05 eV.¹⁷

A systematic investigation of effective masses reveals a similar picture, namely, that sX improves the overall agreement with experiment. In particular, the performance of sX in predicting m_c^Γ is rather remarkable (cf. Table II). Nevertheless, in some cases involving flat bands, significant discrepancies remain (e.g., m_l^X of GaAs and m_l^X of GaSb).

Given this evidence of the applicability of the sX approach to higher-lying CB states the approach is applied to a study of III-V semiconductors, with small to medium-size energy-band gaps, i.e., the compounds AB (A=Al, Ga, In and B=P, As, Sb). The calculations show that:

(1) The $\Gamma-L$ separation varies strongly with the chemical composition. The calculated $\Gamma-L$ separations range from -0.61 eV in AIP (indirect band gap) to 1.21 eV in InAs. The smallest positive $\Gamma-L$ separation for a direct-gap semiconductor is 0.26 eV, obtained for GaSb (cf. Fig. 2).

(2) Within the series of the phosphides, arsenides, and antimonides, the $\Gamma-L$ separation increases nearly linearly with decreasing direct band gap. In contrast, in the series AIP-AlAs-AlSb, GaP-GaAs-GaSb, and InP-InAs-InSb, the $\Gamma-L$ separation increases from the phosphides to the arsenides and decreases from the arsenides to the antimonides (cf. Fig. 2). This trend indicates a stronger chemical influence of the group-V elements on $\Gamma-L$ separation compared with the group-III elements.

(3) For the ternary semiconductors $In_xGa_{1-x}As$ and $In_xGa_{1-x}Sb$, the direct band gap and the $\Gamma-L$ separation vary almost linearly with the lattice parameter ($dE^{\Gamma-\Gamma}/da \approx -3.0$ eV/Å and $dE^{\Gamma-L}/da \approx 1.8$ eV/Å). Hence, the band gap widens upon compression of the material and the $\Gamma-L$ separation diminishes, as discussed in detail by Picozzi *et al.*¹⁹ The value of -3.0 eV/Å determined for $dE^{\Gamma-\Gamma}/da$ in $In_{0.5}Ga_{0.5}As$ may be compared with a value of -3.4 eV/Å obtained by combining the indirectly measured band-gap pressure dependence²⁰ and the bulk modulus²¹ of $In_{0.53}Ga_{0.47}As$ (a composition that is lattice matched to InP). The direct band gap is significantly more sensitive to the lattice parameter than the $\Gamma-L$ separation. The lattice parameter can also be changed by varying the chemical composition, which in turn influences the band gap and $\Gamma-L$ separation.

(4) In ternary alloys such as $In_{1-x}Ga_xAs$ and $In_{1-x}Ga_xSb$, the predicted $\Gamma-L$ separations are influenced strongly by local ordering effects. This is shown clearly in Fig. 2 for $In_{0.75}Ga_{0.25}As$ as discussed by Picozzi *et al.*¹⁹ It is apparent that the composition dependence of the $\Gamma-L$ separation energy is not well described by means of a simple “bowing parameter” like that often used for the direct band gap. Disorder influences the $\Gamma-L$ behavior as well, which adds another dimension of complexity.

(5) The electron effective masses are significantly higher near L than near Γ (cf. Table II).

TABLE I. Computed and experimental energy differences ($\Gamma-L$ and $\Gamma-X$) within the conduction bands of III-V semiconductors (zinc-blende structure). All energies are in eV.

	$\Gamma-L$			$\Gamma-X$		
	LDA	sX	Exp.	LDA	sX	Exp.
AIP	-0.472	-0.610		-1.704	-1.939	-1.125 ^a
GaP	-0.093	-0.192		-0.062	-0.275	
InP	0.846	0.889	0.61, ^a 0.59 ^b	1.175	1.115	0.96, ^a 0.85 ^b
AlAs	0.172	0.004	-0.12 ^c	-0.475	-0.741	-0.901, ^a -0.89 ^c
GaAs	0.600	0.445	0.218, ^a 0.31 ^c	1.156	0.901	0.548, ^a 0.48 ^c
InAs	1.268	1.214	0.74 ^b 1.10 \pm 0.05 ^d	1.967	1.785	1.02, ^b 1.82 \pm 0.05 ^d
AlSb	-0.164	-0.405	-0.057 ^a	-0.246	-0.557	-0.69 ^a
GaSb	0.459	0.261	0.273 ^a 0.084 ^b	1.028	0.748	0.31 ^b
InSb	0.944	0.719	0.51 ^b	1.860	1.533	1.555 ^a 0.83 ^b

^aReference 14.

^bReference 15.

^cReference 16.

^dReference 17.

TABLE II. Computed and measured effective masses in units of the electron mass (conduction masses: m_c , longitudinal and transverse conduction masses: m_l and m_t , heavy hole and light hole masses: m_{hh} and m_{lh}). For InAs, effective density of states masses are defined as: $m^L = [16m_l^L(m_t^L)^2]^{1/3}$ and $m^X = [9m_l^X(m_t^X)^2]^{1/3}$.

	LDA	sX	Exp.
GaAs			
m_c^Γ	0.011	0.055	0.067, ^a 0.063 ^b
m_l^L	1.749	1.870	1.9 ^b
m_t^L	0.099	0.126	0.075 ^b
m_l^X	-0.978	-0.973	1.98, ^c 1.9 ^b
m_t^X	0.272	0.275	0.3, ^c 0.19 ^b
m_{hh}^Γ	0.312	0.323	0.45, ^c 0.51 ^b
m_{lh}^Γ	0.105	0.091	0.085, ^c 0.082 ^b
GaSb			
m_c^Γ	0.066 ^c	0.014	0.0412 ^a
m_l^L	0.080	0.014	
m_t^L	1.745	1.714	0.95 ^b
m_l^X	0.095	0.123	0.11 ^b
m_t^X	-0.721	-0.626	1.51 ^b
m_{hh}^Γ	0.954 ^c	0.691	0.28, ^a 0.22 ^b
InP			
m_c^Γ	0.019	0.089	0.0765, ^a 0.079, ^d 0.081 ^d
m_l^L	0.145	0.180	0.25 ^b
m_t^L	0.402	0.392	0.32 ^b
$m_{hh}^\Gamma(001)$	0.415	0.456	0.56, ^a 0.52, ^d 0.61 ^d
$m_{hh}^\Gamma(111)$	1.011	1.032	0.60, ^a 0.95, ^d 0.63 ^d
$m_{lh}^\Gamma(001)$	0.165	0.172	0.12, ^a 0.104, ^d 0.118, ^d 0.089 ^b
InAs			
$m_c^\Gamma(100)$	0.094 ^c	0.022	0.0231 ^a
$m_c^\Gamma(111)$	0.112 ^c	0.021	
m_l^L	0.862	0.821	0.29 ^b
m^X	1.367	1.254	0.64 ^b
m_{hh}^Γ	0.353 ^c	0.388	0.41 ^b
m_{lh}^Γ	0.046 ^c	0.025	0.026 ^b

^aReference 14.

^bReference 15.

^cReference 16.

^dReference 18.

^eA proper assignment of valence and conduction bands is hampered by the incorrect band overlap in the LDA.

The diagram of the $\Gamma-L$ separation versus the band gap reveals that the InAs-InP tie line might provide the highest $\Gamma-L$ separation of any ternary cubic III-V alloy with a band gap in the vicinity of 0.5 eV (cf. Fig. 2). Compositions near InP_{0.20}As_{0.80} offer band gaps near 0.50 eV, $\Gamma-L$ separations of at least 0.9 eV, and lattice parameters compatible with growth on an InP substrate. Given material quality comparable to that of InGaAs and InGaSb systems with similar band gaps, InPAs should offer higher carrier mobility and lifetime. InPAs alloys should likewise retain low effective masses out to higher dopant densities, a property advantageous for plasma filter applications. At high dopant concentrations, one expects optical band-gap shifts in InPAs to be larger than for other similarly doped alloys. This property can also be used to advantage in TPV devices, in lateral conduction layers, and elsewhere.

In summary, the sX-FLAPW approach is a clear improvement over standard LDA for the description of fundamental band gaps, effective masses and higher-lying states.

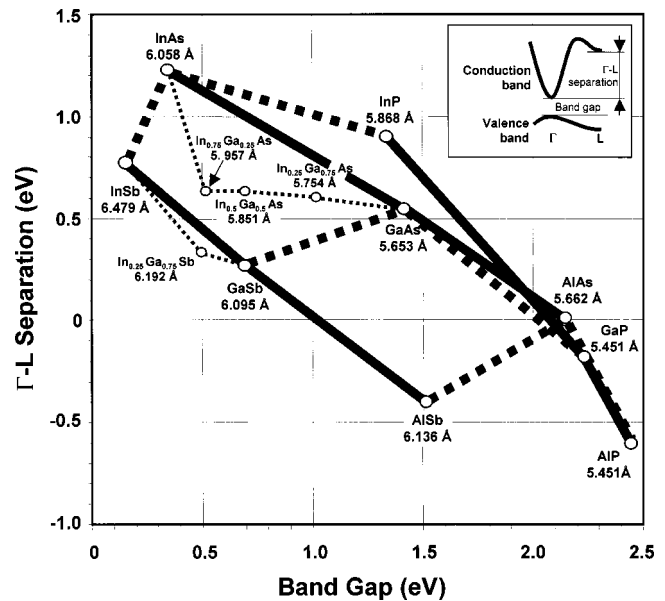


FIG. 2. $\Gamma-L$ separation as a function of the direct-energy-band gap at Γ for nine binary III-V semiconductors AB (A=Al, In, Ga and B=P, As, Sb) and four ternary systems in ordered structures. The solid lines connect binary compounds with the same group-V element and the dashed lines connect ternary compounds with the same group-III element. Experimental lattice constants are given below the name of each compound.

The work at Northwestern University was supported by the NSF (through the Northwestern University Materials Research Center).

¹B. M. Bylander and L. Kleinman, Phys. Rev. B **41**, 7868 (1990).

²A. Seidl, A. Göring, P. Vogl, J. A. Majewski, and M. Levy, Phys. Rev. B **53**, 3764 (1996).

³A. Sher, M. van Schilfgaarde, M. A. Berding, S. Krishnamurthy, and A-B. Chen, MRS Internet J. Nitride Semicond. Res. **4S1**, G5.1 (1999).

⁴J. E. Reynolds, C. B. Geller, G. W. Charache, T. Holden, F. H. Pollak, W. Mannstadt, R. Asahi, and A. J. Freeman, AIP Conf. Proc. **460**, 457 (1999).

⁵S. Adachi, *Physical Properties of III-V Semiconductor Compounds* (Wiley Interscience, New York, 1992), p. 88, and references therein.

⁶J. B. Gunn, Solid State Commun. **1**, 88 (1963).

⁷M. Segev, B. Collings, and D. Abraham, Phys. Rev. Lett. **76**, 3798 (1996).

⁸E. D. Grann, K. T. Tsen, and D. K. Ferry, Phys. Rev. B **53**, 9847 (1996).

⁹M. Shur, *GaAs Devices and Circuits* (Plenum, New York, 1987).

¹⁰W. Wolf, E. Wimmer, S. Massidda, M. Posternak, and C. B. Geller, Bull. Am. Phys. Soc. **43**, 797 (1998).

¹¹R. Asahi, W. Mannstadt, and A. J. Freeman, Phys. Rev. B **59**, 7486 (1999).

¹²E. Wimmer, H. Krakauer, M. Weinert, and A. J. Freeman, Phys. Rev. B **24**, 864 (1981), and references therein.

¹³H. J. F. Jansen and A. J. Freeman, Phys. Rev. B **30**, 561 (1984).

¹⁴A.-B. Chen and A. Sher, *Semiconductor Alloys, Physics and Materials Engineering* (Plenum, New York, 1995), and references therein.

¹⁵*Handbook Series on Semiconductor Parameters*, edited by M. Levenshtein, S. Romyantsev, and M. Shur (World Scientific, New York, 1996), Vol. 1.

¹⁶V. Fiorentini, Phys. Rev. B **46**, 2086 (1992), and references therein.

¹⁷G. W. Charache, D. M. DePoy, J. E. Reynolds, P. F. Baldasaro, K. E. Miyano, T. Holden, F. H. Pollak, P. R. Sharps, M. L. Timmons, C. B. Geller, W. Mannstadt, R. Asahi, A. J. Freeman, and W. Wolf, J. Appl. Phys. **86**, 452 (1999).

¹⁸H. Fu and A. Zunger, Phys. Rev. B **55**, 1642 (1997), and references therein.

¹⁹S. Picozzi, A. Continenza, R. Asahi, W. Mannstadt, A. J. Freeman, W. Wolf, E. Wimmer, and C. B. Geller, Phys. Rev. B **61**, 4677 (2000).

²⁰A. R. Goñi, K. Strössner, K. Syassen, and M. Cardona, Phys. Rev. B **36**, 1581 (1987).

²¹C. S. Menoni, H. D. Hochheimer, and I. L. Spain, Phys. Rev. B **33**, 5896 (1986).